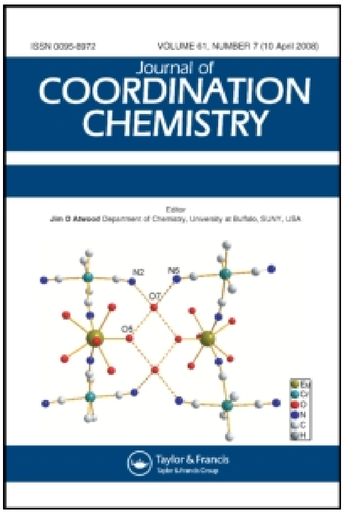

Journal of Coordination Chemistry
Publication details, including instructions for authors and subscription information:
http://www.informaworld.com/smpp/title~content=t713455674

Synthesis, crystal structure, and electrochemistry of [Co{(Me-sal)$_2$dien}(N$_3$)] and [Co{(Me-sal)$_2$dpt}(N$_3$)]

Soraia Meghdadi[a]; Kurt Mereiter[b]; Mehdi Amirnasr[a]; Farzaneh Fadaee[a]; Ahmad Amiri[a]
[a] Department of Chemistry, Isfahan University of Technology, Isfahan 84156-83111, Iran [b] Faculty of Chemistry, Vienna University of Technology, A-1060 Vienna, Austria

To cite this Article Meghdadi, Soraia , Mereiter, Kurt , Amirnasr, Mehdi , Fadaee, Farzaneh and Amiri, Ahmad(2009) 'Synthesis, crystal structure, and electrochemistry of [Co{(Me-sal)$_2$dien}(N$_3$)] and [Co{(Me-sal)$_2$dpt}(N$_3$)]', Journal of Coordination Chemistry, 62: 5, 734 — 744

To link to this Article: DOI: 10.1080/00958970802363966

URL: http://dx.doi.org/10.1080/00958970802363966

Journal of Coordination Chemistry
Vol. 62, No. 5, 10 March 2009, 734–744

Synthesis, crystal structure, and electrochemistry of [Co{(Me-sal)$_2$dien}(N$_3$)] and [Co{(Me-sal)$_2$dpt}(N$_3$)]

SORAIA MEGHDADI†, KURT MEREITER‡, MEHDI AMIRNASR*†,
FARZANEH FADAEE† and AHMAD AMIRI†

†Department of Chemistry, Isfahan University of Technology, Isfahan 84156-83111, Iran
‡Faculty of Chemistry, Vienna University of Technology, Vienna, Getreidemarkt 9/164SC,
A-1060 Vienna, Austria

(*Received 10 April 2008; in final form 2 June 2008*)

The structure, spectroscopic, and electrochemical properties of [Co{(Me-sal)$_2$dien}(N$_3$)] and [Co{(Me-sal)$_2$dpt}(N$_3$)], where (Me-sal)$_2$dien = 2,2′-[1,1′-(3-azapentane-1,5-diyldinitrilo)diethylidyne] diphenolate and (Me-sal)$_2$dpt = 2,2′-[1,1′-(4-azapentane-1,7-diyldinitrilo)diethylidyne] diphenolate, have been investigated. These complexes have been characterized by elemental analyses, IR, UV–Vis, and ^{1}H-NMR spectroscopy. The crystal structures of these complexes have been determined by X-ray diffraction. Complex **1** crystallizes in the triclinic space group $P\bar{1}$, with $a = 7.8443(4)$ Å, $b = 11.0660(5)$ Å, $c = 11.6216(6)$ Å, $\alpha = 73.360(1)^\circ$, $\beta = 76.965(1)^\circ$, $\gamma = 84.436(1)^\circ$ and $Z = 2$. Complex **2** crystallizes in the monoclinic space group $P2_1/n$, with $a = 12.1985(13)$ Å, $b = 10.9332(12)$ Å, $c = 15.2808(16)$ Å, $\beta = 76.965(1)^\circ$ and $Z = 4$. The coordination geometry around cobalt(III) in both complexes is a distorted octahedron. The electrochemical reduction of these complexes at a glassy carbon electrode in acetonitrile indicates that the first reduction corresponding to Co^{III}–Co^{II} is electrochemically irreversible, accompanied by dissociation of the axial Co–N(N$_3$) bond. The second reduction step of Co(II/I) leads to decomposition of the complex. These observations are rationalized based on the structure-function relations.

Keywords: Schiff base; Cobalt(III) azido complexes; Crystal structure; Spectral properties; Cyclic voltammetry

1. Introduction

Schiff bases are useful chelators because of accessibility, structural variety and varied denticity. The structure-function relationship of cobalt Schiff-base complexes has been of importance in the design and application of these complexes [1], and additional hetero ligands contribute to modification of their properties. Pseudohalides are efficient intermediates; azide ion is especially important, forming various networks with different transition and non-transition metal ions [2]. Azide has versatile coordination modes to give monomeric, dimeric and polymeric complexes [3, 4]. Coordination of azide depends on the nature and oxidation state of the central metal ion, as well as nature of the other coordinated ligands [5]. Azide is an inhibitor for several enzymes like ATPases

---

*Corresponding author. Email: amirnasr@cc.iut.ac.ir

Journal of Coordination Chemistry
ISSN 0095-8972 print/ISSN 1029-0389 online © 2009 Taylor & Francis
DOI: 10.1080/00958970802363966

[6], making study of metal-azido complexes [7–15] important for understanding its role in biological processes and supramolecular chemistry.

In continuation of our work on synthesis and structural studies of Co(III) complexes of Schiff bases [16–19], herein we report the syntheses and structural and spectroscopic characterization of $[Co^{III}\{(Me\text{-}sal)_2dien\}(N_3)]$ and $[Co^{III}\{(Me\text{-}sal)_2dpt\}(N_3)]$. X-ray crystal structures have been determined and cyclic voltammetric behavior of these complexes are also discussed.

2. Experimental

2.1. *Materials and physical measurements*

All chemicals were purchased from commercial sources and used as received. Elemental analyses were obtained on a Perkin-Elmer 2400II CHNS-O elemental analyzer. Infrared spectra (KBr pellet) were recorded on a FT-IR JASCO 680 instrument. Electronic spectra were obtained on a JASCO V-570 spectrophotometer. ^{1}H-NMR spectra were measured with a Bruker AVANCE DR X500 spectrometer (500 MHz). Proton chemical shifts are reported in ppm relative to Me_4Si as internal standard. The redox properties of the complexes were studied by cyclic voltammetry. Cyclic voltammograms were recorded using a SAMA Research Analyzer M-500. Three electrodes were utilized in this system, a glassy carbon working electrode, a platinum disk auxiliary electrode and Ag wire as reference electrode. The glassy carbon working electrode (Metrohm 6.1204.110) with 2.0 ± 0.1 mm diameter was cleaned with 1 µm alumina polish prior to each scan. Tetrabutylammonium hexafluorophosphate (TBAH) was used as supporting electrolyte. Acetonitrile was dried over CaH_2. The solutions were deoxygenated by purging with Ar for 5 min. All electrochemical potentials were calibrated *versus* internal $Fc^{+/o}$ ($E^\circ = 0.40$ V *versus* SCE) couple under the same conditions [20].

2.2. *Preparation of $H_2(Me\text{-}sal)_2dien$ ligand*

N,*N*′-*bis*(α-methylsalicylidene)diethylenetriamine ($H_2(Me\text{-}sal)_2dien$) was prepared by following the syntheses outlined for related Schiff bases [21], via condensation of (309 mg, 3.00 mmol) diethylenetriamine (dien) with 2-hydroxyacetophenone (817 mg, 6.00 mmol) at room temperature, and purification by recrystallization from hot chlorobenzene. Yellow crystals were filtered off, washed with cold ethanol and dried under vacuum. Yield: 0.927 g (91%). F.W. for $C_{20}H_{25}N_3O_2 = 339.50$. FT-IR (KBr, cm^{-1}): υ_{max}: 3415–3590 (w, br, OH), 3328 (m, N–H), 1614 (s, C=N). UV–Vis: λ_{max} (nm) (ε, M^{-1}cm^{-1}) (chloroform): 390 (2100), 317 (5200), 251 (54242). ^{1}H-NMR (CD_3OD, 300 MHz): $\delta = 2.46$ (s, 6H, H_c), $\delta = 3.09$ (t, 4H, H_a), $\delta = 3.79$ (t, 4H, H_b), $\delta = 6.66$ (t, 2H, H_e), $\delta = 6.76$ (d, 2H, H_g), $\delta = 7.29$ (dd, 2H, H_f), $\delta = 7.55$ (d, 2H, H_d).

2.3. *Preparation of $H_2(Me\text{-}sal)_2dpt$ ligand*

N,*N*′-*bis*(α-methylsalicylidene)dipropylenetriamine ($H_2(Me\text{-}sal)_2dpt$) was prepared as reported in the literature [22], via condensation of (394 mg, 3.00 mmol) dipropylenetriamine (dpt) with 2-hydroxyacetophenone (817 mg, 6.00 mmol) in ethanol at room temperature, and was purified by recrystallization from hot ethanol. Yield: 1.05 g (95%). F.W. for $C_{22}H_{29}N_3O_2 = 367.50$. FT-IR (KBr, cm^{-1}): υ_{max}: 3300–3400 (m, br, OH), 3295 (s, N–H), 1613 (s, C=N). UV–Vis: λ_{max} (nm) (ε, $M^{-1} cm^{-1}$) (methanol): 389 (2226), 317 (9092), 250 (69935). ^{1}H-NMR (CD_3COCD_3, 500 MHz): $\delta = 7.58$ (2H, d, H_e), 7.26 (2H, t, H_g), 6.78 (2H, d, H_h), 6.75 (2H, t, H_f), 3.63 (4H, t, H_c), 2.71 (4H, t, H_a), 2.34 (6 H, s, H_d), 2.15 (1H, br, N–H), 1.88 (4H, m, H_b).

2.4. *Preparation of [Co{(Me-sal)$_2$dien}(N$_3$)] (1)*

To a stirring solution of $Co(CH_3COO)_2 \cdot 4H_2O$ (0.249 g, 1 mmol) in methanol (25 mL) was added an equimolar amount of the H_2(Me-sal)$_2$dien (0.339 g, 1 mmol). The pink solution turned brown immediately due to formation of [Co^{II}{(Me-sal)$_2$dien}]. To this solution was then added NaN_3 (0.065 g, 1 mmol) and air was bubbled through the reaction mixture for 3 h. The final green-red solution was filtered. Dark red crystals of **1** suitable for X-ray analysis were obtained from the filtrate after 48 h. The crystals were filtered off, washed with cold methanol and dried under vacuum. Yield: 64%. Anal. Calcd for $C_{20}H_{23}CoN_6O_2$ (%): C, 54.80; H, 5.29; N, 19.17. Found: C, 54.53; H, 5.11; N, 19.07. FT-IR (KBr, cm^{-1}): ν_{max}: 2031 (s, N=N=N–), 1597 (s, C=N). UV–Vis (acetonitrile): λ_{max} (nm) (ε, $M^{-1}cm^{-1}$): 616 (515), 375 (2522), 311 (5674). ^{1}H-NMR ($CDCl_3$, 500 MHz): $\delta = 2.58$ (s, 3H, H_c), $\delta = 2.76$ (s, 3H, $H_{c'}$), $\delta = 3.03$–4.85 (m, 8H, $H_{a,a',b,b'}$, NH), $\delta = 6.62$, 6.40 (t, 2H, $H_{e,e'}$), $\delta = 6.58$, 6.28 (d, 2H, $H_{g,g'}$), $\delta = 6.86$, 6.80 (t, 2H, $H_{f,f'}$), $\delta = 7.45$ (d, 2H, $H_{d,d'}$).

2.5. *Preparation of [Co{(Me-sal)$_2$dpt}(N$_3$)] (2)*

This complex was prepared by a procedure similar to that for **1** except that H_2(Me-sal)$_2$dpt ligand was used instead of H_2(Me-sal)$_2$dien. Yield: 70%. F.W. for $C_{22}H_{27}CoN_6O_2 = 466.42$. Anal. Calcd for $C_{22}H_{27}CoN_6O_2$ (%): C, 56.65; H, 5.83; N, 18.02. Found: C, 56.38; H, 5.85; N, 17.83. FT-IR (KBr, cm^{-1}): ν_{max}: 2021.03 (s, N=N=N–), 1594.84 (s,C=N). UV–Vis (acetonitrile): λ_{max} (nm) (ε, $M^{-1}cm^{-1}$): 547 (554), 451 (1694, sh), 357 (2560). ^{1}H-NMR (CD_3CN, 500 MHz): $\delta = 2.63$ (s, 3H, H_d), $\delta = 2.65$ (s, 3H, $H_{d'}$), $\delta = 1.96$–5.22 (m, 12H, $H_{a,a',b,b',c,c'}$), $\delta = 3.50$ (br, NH), $\delta = 6.52$ (m, 2H, $H_{f,f'}$), $\delta = 6.85$, 6.92 (d, 2H, $H_{h,h'}$), $\delta = 6.98$ (m, 2H, $H_{g,g'}$), $\delta = 7.39$, 7.46 (d, 2H, $H_{e,e'}$).

2.6. *X-ray crystallography for 1 and 2*

Dark red crystals suitable for X-ray crystallography were obtained by slow evaporation of methanol solutions of the complexes at room temperature. Thin-slice ω-scans were collected, at 100 K, on a Bruker SMART APEX CCD diffractometer (Mo-Kα radiation, $\lambda = 0.71073$ Å) using SMART [23]. Cell refinement and data reduction were performed with the help of the SAINT program [24]. Crystal data, together with other relevant information on structure determination, are listed in table 1. Empirical absorption corrections, based on redundant intensities, were carried out using SADABS [25]. The structures were solved by direct methods and refined by full matrix

Table 1. Crystal data and structure refinement for **1** and **2**.

Empirical formula	$C_{20}H_{23}CoN_6O_2$ (**1**)	$C_{22}H_{27}CoN_6O_2$ (**2**)
Formula weight	438.37	466.43
Temperature (K)	100(2)	100(2)
Radiation, wavelength (Å)	Mo-Kα, 0.71073	Mo Kα, 0.71073
Crystal system, space group	Triclinic, $P\bar{1}$	Monoclinic, $P2_1/n$
Units cell dimensions (Å, °)		
a	7.8443(4)	12.1985(13)
b	11.0660(5)	10.9332(12)
c	11.6216(6)	15.2808(16)
α	73.360(1)	90
β	76.965(1)	96.386(2)
γ	84.436(1)	90
V (Å^3)	941.10(8)	2025.3(4)
Z	2	4
D_{Calcd} (Mg cm^{-3})	1.547	1.530
Crystal color and size (mm^3)	Red prism, 0.35 × 0.31 × 0.18	Red plate, 0.50 × 0.36 × 0.13
μ (mm^{-1})	0.943	0.881
F(000)	456	976
θ Range (°)	2.92–30.00	2.26–30.01
Index range	$-10 \le h \le 11$ $-14 \le k \le 15$ $-16 \le l \le 16$	$-17 \le h \le 17$ $-15 \le k \le 15$ $-21 \le l \le 21$
Reflection collected	9092	35,205
Independent reflections	5292 [$R_{(\mathrm{int})} = 0.012$]	5878 [$R_{(\mathrm{int})} = 0.032$]
Reflections with $F^2 > 2\sigma$	5061	5452
Absorption correction	Multi-scan	Multi-scan
Max. and min. transmission	0.84 and 0.73	0.89 and 0.59
Data/restraints/parameters	5292/0/267	5878/0/286
Goodness-of-fit on F^2	1.079	1.045
Final R indices [$F^2 > 2\sigma(F^2)$]	$R_1 = 0.0279$ $wR_2 = 0.0778$	$R_1 = 0.0324$ $wR_2 = 0.0849$
R indices (all data)	$R_1 = 0.0288$ $wR_2 = 0.0785$	$R_1 = 0.0353$ $wR_2 = 0.0872$
Largest difference peak, hole (e.Å^{-3})	0.56 and −0.54	0.82 and −0.70

least-squares on F^2 data using SHELXL-97 [26]. Anisotropic displacement parameters were assigned to all non-hydrogen atoms. Most H atoms, except H(2N), were inserted in calculated positions and refined with the riding model. Selected bond distances and angles are given in table 2.

3. Results and discussion

3.1. *Spectroscopic studies*

The IR spectra of the free ligands exhibit a broad band characteristic of OH at 3400–3590 cm^{-1}. The disappearance of this band in the IR spectra of the complexes indicates that the ligand is coordinated as a dianion. The band at 1614 cm^{-1}, characteristic of the imine C=N, in the free ligand is shifted to lower frequencies in the IR spectra of the corresponding complexes, due to coordination of the imine nitrogen [17]. The strong band due to terminal azide appears at 2030 cm^{-1} for [Co$^{\mathrm{III}}$\{(Me-sal)$_2$dien\}(N$_3$)] and 2021 cm^{-1} for [Co$^{\mathrm{III}}$\{(Me-sal)$_2$dpt\}(N$_3$)] [5].

Table 2. Selected bond distances (Å) and angles (°) for **1** and **2**.

Complex	**1**		**2**
Co(1)–O(1)	1.8626(8)	Co(1)–O(1)	1.8917(10)
Co(1)–O(2)	1.8858(8)	Co(1)–O(2)	1.9000(10)
Co(1)–N(1)	1.9026(10)	Co(1)–N(1)	1.9475(12)
Co(1)–N(3)	1.9168(10)	Co(1)–N(3)	1.9664(12)
Co(1)–N(2)	1.9225(10)	Co(1)–N(2)	2.0138(12)
Co(1)–N(4)	1.9788(10)	Co(1)–N(4)	1.9561(12)
N(4)–N(5)	1.1925(15)	N(4)–N(5)	1.2062(17)
N(5)–N(6)	1.1565(15)	N(5)–N(6)	1.1559(18)
O(1)–Co(1)–N(1)	94.78(4)	O(1)–Co(1)–O(2)	176.37(4)
O(2)–Co(1)–N(3)	87.84(4)	O(1)–Co(1)–N(1)	89.82(5)
N(1)–Co(1)–N(3)	169.20(4)	O(2)–Co(1)–N(3)	87.54(5)
O(1)–Co(1)–N(2)	177.27(4)	N(1)–Co(1)–N(3)	178.39(5)
N(1)–Co(1)–N(2)	87.15(4)	N(1)–Co(1)–N(2)	90.03(5)
N(3)–Co(1)–N(2)	82.88(4)	N(3)–Co(1)–N(2)	88.38(5)
O(2)–Co(1)–N(4)	178.01(4)	N(2)–Co(1)–N(4)	178.89(5)
N(6)–N(5)–N(4)	175.17(12)	N(6)–N(5)–N(4)	176.58(15)

The electronic absorption spectrum of H_2Me-saldien in chloroform consists of two relatively intense bands centered at 251 and 320 nm, assigned to $\pi \rightarrow \pi^*$ transitions of the benzene ring of salicylaldehyde and the azomethine group, respectively, and a third band at 397 nm, corresponding to $n \rightarrow \pi^*$ which, upon coordination of the ligand, disappears from the UV–Vis spectrum of its cobalt complex. The intraligand $\pi \rightarrow \pi^*$ transition of the azomethine is red shifted by about 55 nm in the corresponding cobalt complex and appears at 375 nm. The first d → d transition in the spectrum of **1** appears at 616 nm [19].

The electronic absorption spectrum of H_2Me-saldpt in methanol shows features similar to those for H_2Me-saldien, two $\pi \rightarrow \pi^*$ transitions at 250 and 337 nm, and a third band at 362 nm corresponding to $n \rightarrow \pi^*$ excitation. The $n \rightarrow \pi^*$ band is absent in the spectrum of the cobalt complex. In addition, the intraligand $\pi \rightarrow \pi^*$ transition of the azomethine is red shifted by about 45 nm, and appears at 381 nm. The first d → d transition in the corresponding cobalt complex **2** appears at 547 nm.

The d-d transition **2** appears at shorter wavelength than **1** by ~70 nm, presumably due to a more efficient overlap between the Me-saldpt donor orbitals and the d-orbitals of cobalt. This stems from a structurally less demanding conformation of Me-saldpt in **2** (bite angles of 90.03° and 88.38°) compared to that of Me-saldien in **1** (bite angles of 87.15° and 82.88°) (*vide infra*).

The ^{1}H-NMR spectral data of **1** and **2** are given in the experimental section. There are three main features in the spectra of the complexes: (i) two singlets at 2.58 (H_c) and 2.76 ppm ($H_{c'}$) in **1** corresponding to different methyl protons adjacent to the iminic nitrogens (CH_3(N); two closely spaced singlets at 2.63 (H_d) and 2.65 ppm ($H_{d'}$) in **2** corresponding to the two almost identical (CH_3(N) protons; (ii) signals due to the aliphatic protons of the ethylene and propylene chelate rings are multiplets in the range 3.03 to 4.85 ppm in **1** and 1.96–5.22 ppm in **2**. The secondary amine NH is a broad multiplet at 4.33 ppm in **1** and at 3.51 ppm in **2** due to different geometries of the two complexes and the extent of hydrogen bonding (*vide infra*); (iii) aromatic protons of the phenyl rings as complex multiplets are between 6.28 to 7.45 ppm in **1** and 6.52 to 7.46 ppm in **2**. These signals correlate well with those reported for related complexes [19].

3.2. *Description of structures*

3.2.1. Crystal structure of [Co^{III}{(Me-sal)$_2$dien}(N$_3$)] (1). The molecular structure of [Co^{III}{(Me-sal)$_2$dien}(N$_3$)] (**1**) with atom numbering is presented in figure 1, and selected bond angles and distances are listed in table 2. The complex crystallizes in triclinic space group $P\bar{1}$ and can be described as a distorted octahedron, *cis* for two O and meridional for three N as compared to [Co(Mesal)$_2$tren)]Cl · CH$_3$OH · H$_2$O, which is *cis* for two O and facial for three N [27]. The O2 (phenolate-O atom) and N4 (azide group) are *trans* to each other. The Co–O(phenolate), Co–N(imine), and Co–N(secondary amine) bond lengths are comparable with those observed in related Co(III) complexes [27, 28]. The Co1–N4 bond length is 1.9788(10) Å, and the terminal azide is almost linear with the N6–N5–N4 angle being 175.17(12)°, in agreement with previous reports [5, 29].

From the three *trans* angles, two {O2–Co1–N4, 178.01(4)° and O1–Co1–N2, 177.27(4)°} are close to ideal and the other {N1–Co1–N3, 169.20(4)°} deviates significantly. The two chelate bite angles formed by the two imine-N and the secondary amine-N of the Schiff base {N1–Co1–N2, 87.15(4)°; N3–Co1–N2, 82.88(4)°} are not identical. Similarly, the six-membered chelate rings formed by the phenolate-O and the imine-N atoms have different bite angles {O1–Co1–N1, 94.78(4)°; O2–Co1–N3, 87.84(4)°}. Relatively strong intermolecular hydrogen bonding between the secondary amine NH of one molecule and the N(N6) azido of the neighboring molecule {N2–H · · · N6, 2.14(2) Å} is observed. The neutral complexes are linked by hydrogen bonds N2–H · · · N6 into chains parallel to the *a*-axis.

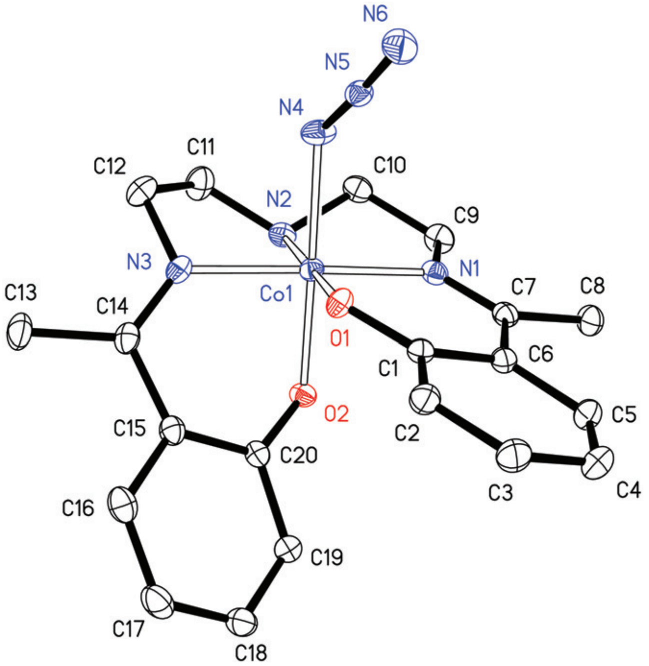

Figure 1. ORTEP diagram of [Co^{III}{(Me-sal)$_2$dien}(N$_3$)] with the atom numbering scheme, drawn with 50% probability ellipsoids and H-atoms omitted.

3.2.2. Crystal structure of [Co^{III}{(Me-sal)$_2$dpt}(N$_3$)] (2). The molecular structure of [Co^{III}{(Me-sal)$_2$dpt}(N$_3$)] with atom numbering is presented in figure 2 and selected bond distances and angles are listed in table 2. The complex crystallizes in monoclinic space group *P*2$_1$/n as a distorted octahedron. Similar to [Co{(Mesal)$_2$dpt}(py)]PF$_6$ [30], **2** is *trans* for two O and meridional for three N. However, it is different from [Co(sal)$_2$dpt(CH$_3$COO)], which is *cis* for two O and meridional for three N [31]. The Co–O(phenolate), Co–N(imine), and Co–N(secondary amine) bond lengths are comparable with related Co(III) complexes [29]. The Co1–N4 bond length is 1.9561(12) Å and the terminal azide is almost linear with the N6–N5–N4 angle being 176.58(15)°, in accord with reported data [5, 29].

From the three *trans* angles, two {N2–Co1–N4, 178.89(5)° and N1–Co1–N3, 178.39(5)°} are close to ideal and one {O1–Co1–O2, 176.37(4)°} deviates slightly. The two chelate bite angles formed by the two imine-N and the secondary amine-N of the Schiff base {N1–Co1–N2, 90.03(5)°; N3–Co1–N2, 88.38(5)°} are almost identical and close to ideal. As in **1**, the six-membered chelate rings formed by the phenolate-O and the imine-N atoms have different bite angles {O1–Co1–N1, 89.82(5)°; O2–Co1–N3, 87.54(5)°}, however, the deviation from ideal is less significant than in **1**. The central amino group (N2) forms a comparatively long intramolecular hydrogen bond to O2 as acceptor {N2–H···O2, 2.62(2) Å}. The terminal N6 of the azide exhibits a weak interaction with a CH$_3$ group of a neighboring complex.

From the structure analysis of **1** and **2**, it is clear that the conformations adopted by (Me-sal)$_2$dien and (Me-sal)$_2$dpt are different. The coordination about Co is pseudo-octahedral, with angles between neighboring vertices varying from 82.88° to 95.53° in **1** and 86.91° to 92.82° in **2**. The deviation from ideal is less significant for **2** due to the less demanding structure of (Me-sal)$_2$dpt as compared to that of (Me-sal)$_2$dien. This difference is also shown in redox potentials of the two complexes (*vide infra*).

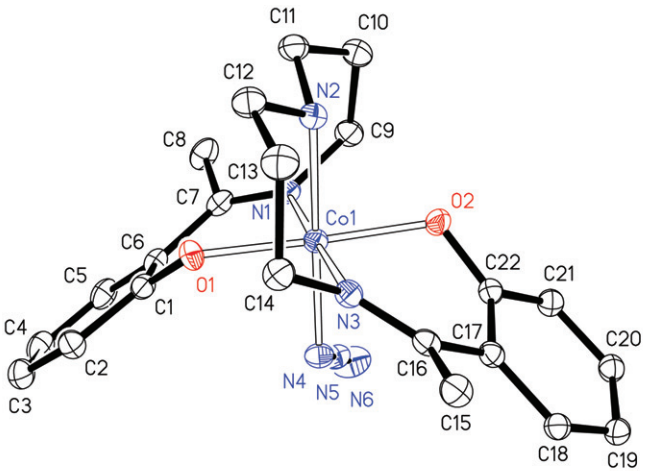

Figure 2. ORTEP diagram of [Co^{III}{(Me-sal)$_2$dpt}(N$_3$)] with the atom numbering scheme, drawn with 50% probability ellipsoids and H-atoms omitted.

3.3. *Electrochemical studies*

The cyclic voltammograms of $[Co^{III}\{(Me\text{-}sal)_2dien\}(N_3)]$ and $[Co^{III}\{(Me\text{-}sal)_2dpt\}(N_3)]$ were obtained at 25°C under an argon atmosphere using acetonitrile solution containing $0.1\,mol\,dm^{-3}$ TBAH as supporting electrolyte and complex concentrations of 4×10^{-3} M. The ligands are electro-inactive from +0.7 to −2.2 V. The redox properties of the two Co(III) complexes exhibit grossly similar features consisting of an electrochemically irreversible Co^{III}/Co^{II} reduction at ca −0.951 V (peak separation ~670 mV) for **1** (figure 3) and ca −0.989 V (peak separation ~818 mV) for **2** (figure 4), due to:

$$[Co^{III}\{(Me-sal)_2dien\}(N_3)] + e \rightarrow [Co^{II}\{(Me-sal)_2dien\}] + N_3^-$$

Since one electron is added to the antibonding d_z^2 orbital, the reduction is accompanied by loss of N_3^- [17, 32]. Contrary to many cobalt complexes of tetradentate (N_2O_2) Schiff-base ligands which undergo electrochemically reversible reduction in a more negative potential region corresponding to the simple one electron process $[Co^{II}L] + e^- \rightarrow [Co^{I}L]^-$, [17, 32], the second reduction process for **1** ($E_{pc} = -2.029$ V) and **2** ($E_{pc} = -2.140$ V) is irreversible.

In the context of the structural effects on the electrochemical properties of Co(III) Schiff-base complexes, the observed electrochemical behavior of **1** and **2** provides some interesting features: (i) The two Co^{III}–Co^{II} and Co^{II}–Co^{I} reduction processes occur at more positive potentials in **1** relative to **2**. The deviation of the coordination angles from ideal (90°) is more pronounced in **1** than **2**, rendering the Co more electron deficient in **1**, and in turn the reduction occurs at a more positive potential. (ii) The structural demands imparted by $(Me\text{-}sal)_2dien$ and $(Me\text{-}sal)_2dpt$ are considerable compared to most tetradentate N_2O_2 Schiff-base ligands. The planar $[Co^{I}L]^-$ intermediate is stable for tetradentate ligands of small structural strain, and as expected, a reversible Co^{II}/Co^{I} process is observed. This process is irreversible, however, for **1** and **2**, presumably due to the instability imposed by the structurally demanding pentadentate ligands on $[Co^{I}L]^-$. Figure 5 shows the irreversible Co^{II}/Co^{I} reduction in **2**.

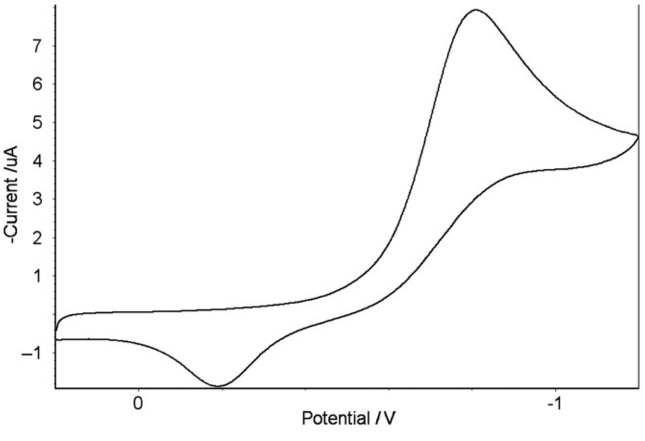

Figure 3. Cyclic voltammogram corresponding to Co(III) → Co(II) for $[Co^{III}\{(Me\text{-}sal)_2dien\}(N_3)]$ in acetonitrile at 293 K. Scan rate: $100\,mV\,s^{-1}$. $c = 2 \times 10^{-4}$ M.

4. Conclusion

The structures, spectroscopic and electrochemical properties of [Co{(Me-sal)$_2$dien}(N$_3$)], **1** and [Co{(Me-sal)$_2$dpt}(N$_3$)], **2**, have been investigated. The spatial positions of the donor atoms are different in these two complexes and the deviation of the coordination angles from ideal (90°) is more pronounced in **1** relative to **2**. The d-d transition in the electronic absorption spectrum of **2** appears at shorter wavelength than **1** by ~70 nm, presumably due to a more efficient overlap between the Me-saldpt donor orbitals and the d-orbitals of cobalt **2**. The reduction processes occur at more positive potentials in **1** relative to **2**, indicating that the Co atom is more electron deficient in **1**

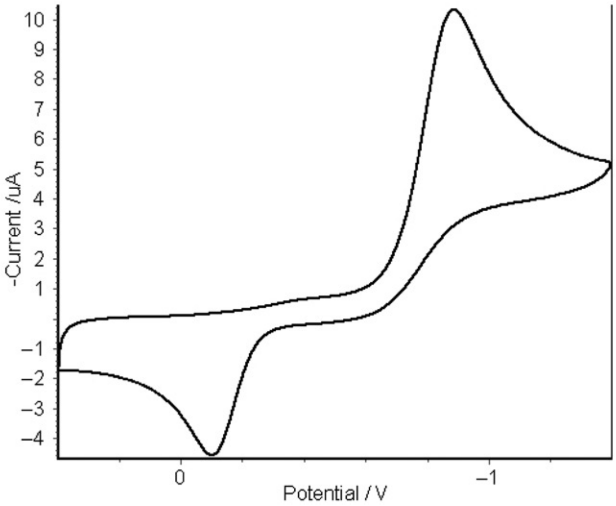

Figure 4. Cyclic voltammogram corresponding to Co(III) → Co(II) for [Co^{III}{(Me-sal)$_2$dpt}(N$_3$)] in acetonitrile at 293 K. Scan rate: 100 mV s^{-1}. $c = 2 \times 10^{-3}$ M.

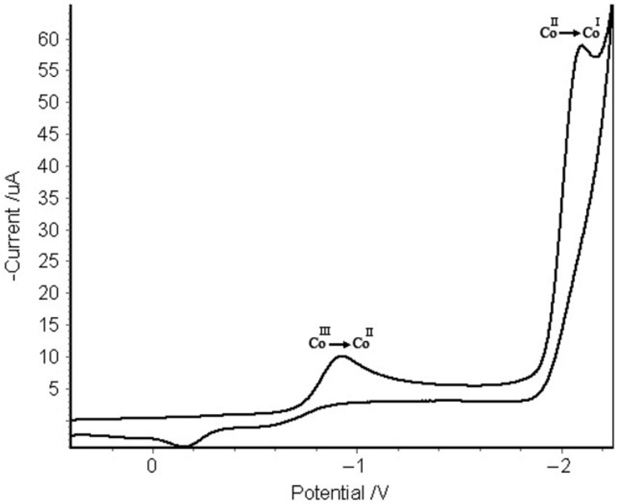

Figure 5. Cyclic voltammogram corresponding to Co(III) → Co(II) and Co(II) → Co(I) for [Co^{III} {(Me-sal)$_2$dpt}(N$_3$)] in acetonitrile at 293 K. Scan rate: 100 mV s^{-1}. $c = 2 \times 10^{-3}$ M.

due to the more strained Me-saldien in **1** compared to Me-saldpt in **2**. Contrary to complexes of most tetradentate N_2O_2 Schiff bases in which the Co^{II}/Co^{I} process is reversible, due to the stability of the $[Co^{I}L]^{-}$ intermediate, this process is irreversible for **1** and **2** presumably due to the instability imposed by the structurally demanding pentadentate ligands on the $[Co^{I}L]^{-}$ intermediate.

Supplementary material

Crystallographic data for **1** and **2** have been deposited with the Cambridge Crystallographic Data Centre as supplementary publications, CCDC reference numbers 683385 and 683386. These data can be obtained free of charge via http://www.ccdc.cam.ac.uk/conts/retrieving.html (or from the Cambridge Crystallographic Data Centre, 12 Union Road, Cambridge CB2 1EZ, UK; Fax: (+44) 1223-336-033; or Email: deposit@ccdc.cam.ac.uk).

Acknowledgement

Partial support of this work by the Isfahan University of Technology Research Council is gratefully acknowledged.

References

[1] P.G. Cozzi. *Chem. Soc. Rev.*, **33**, 410 (2004).
[2] R. Ghosh, S.H. Rahaman, Ch.-N. Lin, T.-H. Lu, B.K. Ghosh. *Polyhedron*, **25**, 3104 (2006).
[3] E. Ruiz, J. Cano, S. Alvarez, P. Alemany. *J. Am. Chem. Soc.*, **120**, 11122 (1998).
[4] H.-Y. Wu, H.-Q. An, B.-L. Zhu, Sh.-R. Wang, Sh.-M. Zhang, Sh.-H. Wu, W.-P. Huang. *Inorg. Chem. Commun.*, **10**, 1132 (2007).
[5] S.S. Massoud. *Polyhedron*, **18**, 2287 (1999).
[6] A.F. Knowles, A.K. Nagy. *Eur. J. Biochem.*, **262**, 349 (1999).
[7] S.H. Rahaman. *Inorg. Chem. Commun.*, **8**, 1031 (2005).
[8] M.A.S. Goher, F.A. Mautner. *Polyhedron*, **17**, 1561 (1998).
[9] J.P. Costes, F. Dahan, J. Ruiz, J.P. Laurent. *Inorg. Chim. Acta*, **239**, 53 (1995).
[10] M.G.B. Drew, J. Hunter, D.J. Marrs, J. Nelson, C. Harding. *J. Chem. Soc., Dalton Trans.*, **22**, 3235 (1992).
[11] P. Chaudhuri, T. Weyhermuller, E. Bill, K. Wieghardt. *Inorg. Chim. Acta*, **252**, 195 (1996).
[12] J. Ribas, M. Monfort, B.K. Ghosh, R. Cortés, X. Solans, M. Font-Bardia. *Inorg. Chem.*, **35**, 864 (1996).
[13] R. Vicente, A. Escuer. *Polyhedron*, **14**, 2133 (1995).
[14] A. Escuer, R. Vicente, M.S. El-Fallah, X. Solans, M. Font-Bardia. *Inorg. Chim. Acta*, **247**, 85 (1996).
[15] S.S. Massoud. *Polyhedron*, **13**, 3127 (1994).
[16] M. Amirnasr, K.J. Schenk, A.R. Gorji, R. Vafazadeh. *Polyhedron*, **20**, 695 (2001).
[17] M. Amirnasr, R. Vafazadeh, A. Mahmoudkhani. *Can. J. Chem.*, **80**, 1196 (2002).
[18] M. Amirnasr, V. Langer, N. Rasouli, M. Salehi, S. Meghdadi. *Can. J. Chem.*, **83**, 2073 (2005).
[19] K.J. Schenk, S. Meghdadi, M. Amirnasr, M.H. Habibi, A. Amiri, M. Salehi, A. Kashi. *Polyhedron*, **26**, 5448 (2007).
[20] N.G. Connelly, W.E. Geiger. *Chem. Rev.*, **96**, 877 (1996).
[21] L. Sacconi, I. Bertini. *J. Am. Chem. Soc.*, **88**, 5180 (1966).
[22] M. Amirnasr, K.J. Schenk, S. Meghdadi, M. Morshedi. *Polyhedron*, **25**, 671 (2006).
[23] Bruker program *SMART*, version 5.629; Bruker AXS Inc, Madison, WI (2003).
[24] Bruker program *SAINT*, version 6.45; Bruker AXS Inc, Madison, WI (2003).

[25] Bruker program *SADABS*, version 2.10; Bruker AXS Inc, Madison, WI (2003).
[26] G.M. Sheldrick. *SHELXL-97, Program System for Crystal Structure Determination*, University of Göttingen, Germany (1997).
[27] H.-Y. Fu, J.-M. Dou, D.-C. Li, D.-Q. Wang. *Acta Cryst*., **E62**, m2213 (2006).
[28] S. Meghdadi, K.J. Schenk, M. Amirnasr, F. Fadaee. *Acta Cryst*., **E64**, m479 (2008).
[29] S. Sreesha, M.R.P. Kurup. *J. Chem. Cryst*., **37**, 31 (2007).
[30] S. Meghdadi, J.-C. Daran, M. Amirnasr, M. Morshedi. *Acta Cryst*., **E63**, m982 (2007).
[31] O.Q. Munro, S. Govender. *Acta Cryst*., **C63**, m150 (2007).
[32] A. Bottcher, T. Takeuchi, K.I. Hardcastle, T.J. Meade, H.B. Gray. *Inorg. Chem*., **36**, 2498 (1997).